CHEMISTRY OF MATERIALS

Article

pubs.acs.org/cm

Remote Stabilization of Copper Paddlewheel Based Molecular Building Blocks in Metal−Organic Frameworks

Wen-Yang Gao,[†] Rong Cai,[‡] Tony Pham,[†] Katherine A. Forrest,[†] Adam Hogan,[†] Patrick Nugent,[†] Kia Williams,[†] Lukasz Wojtas,[†] Ryan Luebke,[§] Łukasz J. Weseliński,[§] Michael J. Zaworotko,[†] Brian Space,[†] Yu-Sheng Chen,[∥] Mohamed Eddaoudi,*[,§] Xiaodong Shi,*[,‡] and Shengqian Ma*[,†]

[†]Department of Chemistry, University of South Florida, 4202 East Fowler Avenue, CHE205, Tampa, Florida 33620, United States

[‡]Department of Chemistry, West Virginia University, Morgantown, West Virginia 26506, United States

[§]Functional Materials Design, Discovery and Development Research Group (FMD3), Advanced Membranes and Porous Materials Center, Division of Physical Sciences and Engineering, King Abdullah University of Science and Technology (KAUST), Thuwal 23955-6900, Kingdom of Saudi Arabia

[∥]ChemMatCARS, Center for Advanced Radiation Sources, The University of Chicago, 9700 S. Cass Avenue, Argonne, Illinois 60439, United States

Supporting Information

ABSTRACT: Copper paddlewheel based molecular building blocks (MBBs) are ubiquitous and have been widely employed for the construction of highly porous metal−organic frameworks (MOFs). However, most copper paddlewheel based MOFs fail to retain their structural integrity in the presence of water. This instability is directly correlated to the plausible displacement of coordinating carboxylates in the copper paddlewheel MBB, $[Cu_2(O_2C-)_4]$, by the strongly coordinating water molecules. In this comprehensive study, we illustrate the chemical stability control in the **rht**-MOF platform via strengthening the coordinating bonds within the triangular inorganic MBB, $[Cu_3O(N_{4-x}(CH)_xC-)_3]$ (x = 0, 1, or 2). Remotely, the chemical stabilization propagated into the paddlewheel MBB to afford isoreticular **rht**-MOFs with remarkably enhanced water/chemical stabilities compared to the prototypal **rht**-MOF-1.

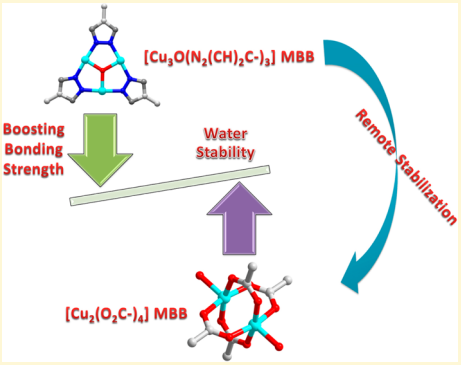

INTRODUCTION

Metal−organic frameworks (MOFs), composed of polytopic organic ligands linking metal ions or metal clusters, have emerged as a new class of functional and tunable porous solid-state materials.[1] Resultantly, MOFs have witnessed tremendous interest from industry and academia alike, due to their unparalleled modularity through successful use of crystal engineering and/or reticular chemistry strategies.[2] In principal, a material designer could target a desired structure by judiciously selecting the requisite geometry, directionality, and connectivity of the organic and inorganic based molecular building blocks (MBBs) to match the vertex figures of a given net.[3] Accordingly, establishment of reaction conditions for a given MOF platform offers the potential to access MOFs with fine-tuned properties (e.g., controlled pore size, ultra-large surface area, tuned pore surface functionality, and enhanced chemical stability).[3] These unique features offer great prospective pertaining to gas storage,[4] separation,[5] CO_2 capture,[6] sensors,[7] catalysis,[8] and various other applications.[9]

Among various inorganic MBBs encountered in MOFs,[3] the copper paddlewheel based MBB, $[Cu_2(O_2C-)_4]$, is ubiquitous and has been widely employed for the construction of highly porous MOFs as exemplified in many prototypal MOF platforms, e.g., **tbo**-MOFs (HKUST-1),[10] **nbo**-MOFs (MOF-505),[11] and **rht**-MOFs (**rht**-MOF-1).[12] Nevertheless, most copper paddlewheel based MOFs remain unexplored industrially due to their instability in relevant environments which contain moisture,[13] water,[14] steam,[15] and acidic media.[16] Such drawbacks restrict their application in many industrial areas where zeolites have shown a major impact.[17] Presumably, the copper paddlewheel is the most susceptible position for structural degradation, of associated MOFs, by water molecules, as suggested by recent studies.[14b,18] Accordingly, it is critical to enhance the paddlewheel stability in order to achieve associated practical MOFs.

Various strategies for imparting MOF water stability, in the context of adsorption applications, have been highlighted and detailed in a recent review article.[19] Primarily, these strategies are based on tuning the ligands' properties (e.g., hydrophobicity and steric factors) in order to enhance the metal−ligand bonds and/or shield the inorganic cluster from water exposure.[19] It is worth noting that copper paddlewheels are relatively less stable

Received: January 9, 2015
Revised: February 28, 2015
Published: March 13, 2015

DOI: 10.1021/acs.chemmater.5b00084
Chem. Mater. 2015, 27, 2144−2151

Scheme 1. Illustration of the Arrangement of Six Carboxylates in a Hexagonal Motif in (a) rht-MOF-1; (b) Various Functional Hexatopic Carboxylate Ligands; (c) rht-MOF-tri; (d) rht-MOF-pyr

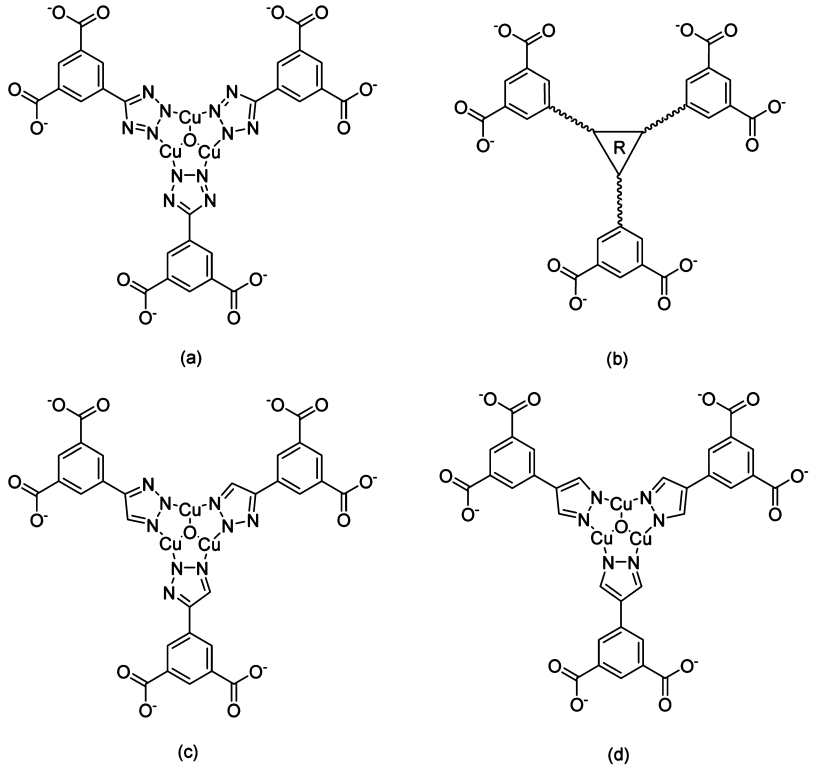

Table 1. Crystal Data and Structure Refinement of rht-MOFs

	rht-MOF-1	**rht**-MOF-tri	**rht**-MOF-pyr
formula	$C_{27}H_9Cu_6N_{13}O_{39.5}$	$C_{30}H_{12}Cu_6N_9O_{23.5}$	$C_{33}H_{15}Cu_6N_6O_{19}$
fw	1527.6	1255.73	1180.75
crystal system	cubic	cubic	cubic
space group	$Fm\bar{3}m$	$Fm\bar{3}m$	$Fm\bar{3}m$
a, Å	44.358(8)	44.271(2)	44.588(3)
b, Å	44.358(8)	44.271(2)	44.588(3)
c, Å	44.358(8)	44.271(2)	44.588(3)
α, deg	90	90	90
β, deg	90	90	90
γ, deg	90	90	90
V, Å^3	87280(27)	86769(7)	88647(12)
Z	192	32	32
θ range for data collection	2.05−19.23	1.20−14.24	0.75−15.99
d_{calcd}, g/cm^3	0.93	0.769	0.708
GOF	1.084	1.079	1.080
R1, wR2	0.1085, 0.1933	0.1083, 0.2757	0.0751, 0.2133

than their nickel counterparts, as suggested by the comparative hydrolysis studies.[20]

In our continuous pursuit to enhance the copper paddlewheel based MOF stability, we explored the effect of heterofunctional ligands on the relationship between the resultant inorganic MBBs. Namely, we elected to study the **rht**-MOF platform as it encloses the copper paddlewheel MBB in addition to a modular triangular inorganic MBB $[Cu_3O(N_{4-x}(CH)_xC-)_3]$ (x = 0, 1, or 2). This platform allows tuning the basicity of the coordinating moiety forming the triangular MBB (functionalizing via a crystal engineering approach) and subsequently exploring its impact on copper paddlewheel water/chemical stability.

rht-MOFs have been intensively explored over the past few years[12,21] as their structure consists of multiple fine-tunable cages and their underlying (3,24)-connected **rht** topology precludes interpenetration. The first **rht**-MOF (**rht**-MOF-1) was reported in 2008,[12] and is based on the assembly of two independent inorganic MBBs, the copper paddlewheel and the triangular $[Cu_3O(N_4C-)_3]$. The trigonal inorganic MBB serves to position three 5-tetrazolylisophthalate ligands in a structural motif resembling a hexacarboxylate building block (Scheme 1a), peripherally exposing six carboxylates from three coplanar isophthalate moieties. Over 40 **rht**-MOF structures have been reported based on tetrazolate ligands or purely organic trigonal cores having three isophthalate or associated derivatives

DOI: 10.1021/acs.chemmater.5b00084
Chem. Mater. 2015, 27, 2144−2151

(Scheme 1b). Many of these **rht**-MOFs have been extensively investigated for gas storage and CO_2 capture.[12,21] Indeed, **rht**-MOFs exhibit exceptionally high surface areas and relatively high uptakes for adsorbed hydrogen, methane, and CO_2.[21] Indeed, the current record for experimental BET surface area is held by the **rht**-MOF, NU-110.[21o] Nevertheless, like most MOFs,[13−16] they suffer from poor water stability and chemical stability.[17] Given that the copper paddlewheel is the most susceptible position for degradation by hydrolysis,[14b,18] we speculate that boosting the bonding strength between the organic MBBs and the trigonal inorganic MBBs could synergistically and remotely stabilize the copper paddlewheel MBBs, which in return leads to the enhancement of water stability of the **rht**-MOF platform. Considering the very strong bonding between transition metal ions and azolate groups, as observed in some water/chemical stable MOFs,[16,22] we replaced the tetrazole moiety of 5-tetrazolylisophthalic acid with 1,2,3-triazole (Scheme 1c) or pyrazole (Scheme 1d) and obtained two new **rht**-MOFs, **rht**-MOF-tri (tri is short for triazolate) and **rht**-MOF-pyr (pyr is short for pyrazolate) that are isostructural with **rht**-MOF-1. As we expected, the substitution of one or two atoms resulted in enhanced water, moisture, steam, and chemical stabilities.

RESULT AND DISCUSSION

Crystal Structure Description. Single-crystal X-ray diffraction reveals that both **rht**-MOF-tri and **rht**-MOF-pyr crystallize in the same space group, $Fm\bar{3}m$, as **rht**-MOF-1 with a = 44.271(2) Å (**rht**-MOF-tri) and a = 44.588(3) Å (**rht**-MOF-pyr) (vs 44.358(8) Å in **rht**-MOF-1) (Table 1). As expected, **rht**-MOF-tri and **rht**-MOF-pyr display the same topology as **rht**-MOF-1 and isoreticular analogues such as NOTT-112,[21c] PCN-61,[21d] and NU-100.[21g] $[Cu_3O(N_3CHC-)_3]$ in **rht**-MOF-tri and $[Cu_3O(N_2(CH)_2C-)_3]$ in **rht**-MOF-pyr serve as 3-connected nodes that link six $[Cu_2(O_2C-)_4]$ paddlewheel MBBs through six carboxylate groups of three 5-(1*H*-1,2,3-triazol-4-yl)isophthalate (taip) or 5-(1*H*-pyrazol-4-yl)-isophthalate (paip) ligands, thus affording the expected (3, 24)-connected **rht** network topology (Figure 1). **rht**-MOF-tri and **rht**-MOF-pyr, therefore, contain three large polyhedral cages: a small rhombihexahedral (or rhombicuboctahedral) cage formed by 24 functionalized isophthalate ligands linked by 12 $[Cu_2(O_2C-)_4]$ paddlewheel MBBs (Figure 1a); a bevelled octahedral cage defined by 8 $[Cu_3O(N_3C_2-)_3]$ or $[Cu_3O(N_2C_3-)_3]$ trimers and 24 $[Cu_2(O_2C-)_4]$ paddlewheel MBBs (Figure 1b); a bevelled tetrahedral cage enclosed by 4 $[Cu_3O(N_3C_2-)_3]$ or $[Cu_3O(N_2C_3-)_3]$ trimers and 12 $[Cu_2(O_2C-)_4]$ paddlewheel MBBs (Figure 1c). Both **rht**-MOF-tri and **rht**-MOF-pyr are highly porous and have a comparable solvent accessible volume of ~72% calculated by PLATON.[23]

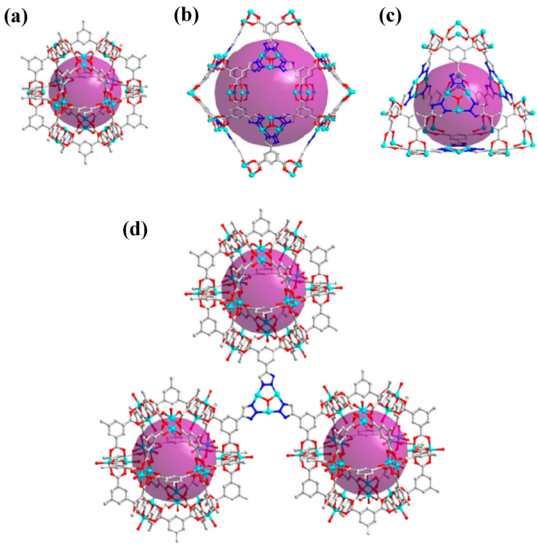

Figure 1. (a) The small rhombihexahedral cage; (b) the bevelled octahedral cage; (c) the bevelled tetrahedral cage; (d) the C_3 symmetric building moiety of **rht**-MOF-tri and **rht**-MOF-pyr.

Evaluation of Water/Chemical Stabilities by Powder X-ray Diffraction (PXRD) Studies. We systematically evaluated the water stability of **rht**-MOF-1, **rht**-MOF-tri, and **rht**-MOF-pyr. As shown in Figure 2, **rht**-MOF-1 was observed

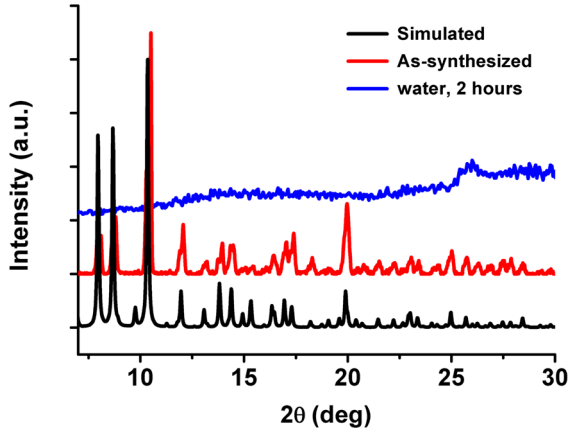

Figure 2. PXRD patterns of **rht**-MOF-1 for simulated plot, as-synthesized sample, and sample after being immersed in water for 2 h.

to decompose after being immersed in water for less than 2 h. Poor water stability was also observed for other **rht**-MOFs based upon hexatopic carboxylate ligands, such as PCN-66[21d] that is constructed from 5,5′,5″-(4,4′,4″-nitrilotris(benzene-4,1-diyl)tris(ethyne-2,1-diyl))triisophthalate (ntei) (Scheme S1a, Supporting Information) and $[Cu_{24}(TPBTM^{6-})_8(H_2O)_{24}]$[21h] that is built from *N*,*N*′,*N*″-tris(isophthalyl)-1,3,5-benzenetricarboxamide (tpbtm) (Scheme S1b), neither of which retained their crystallinity after being immersed in water for 1 h (Figures S1, S2, Supporting Information). The isophthalic moieties are covalently connected in the hexatopic ligands (ntei and tpbtm) and thus are not prone to hydrolysis. The observed poor water stability for PCN-66 and $[Cu_{24}(TPBTM^{6-})_8(H_2O)_{24}]$ should be attributed to the dissociation of the copper paddlewheel MBBs as a result of water attack.[14b,18] Similarly, the decomposition of **rht**-MOF-1 could be ascribed to the breakdown of the copper paddlewheel MBBs, although there is no information for the stability of the trigonal inorganic MBBs in the presence of water.

In contrast with **rht**-MOF-1, **rht**-MOF-tri crystals were soaked in water for 48 h, and PXRD studies revealed no significant changes in the diffraction patterns (Figure 3). However, the extension of water soaking time to 4 days leads to the vanishing and broadening of PXRD peaks, indicative of decomposition (Figure 3). In comparison, **rht**-MOF-pyr can retain its crystallinity after immersion in water for 15 days, as evidenced by no significant changes in the PXRD pattern (Figure 4). These results suggest the following order of

DOI: 10.1021/acs.chemmater.5b00084
Chem. Mater. 2015, 27, 2144−2151

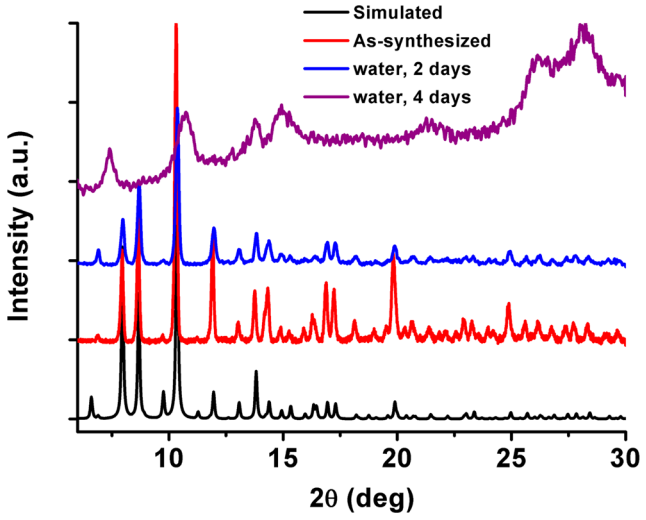

Figure 3. PXRD patterns of **rht**-MOF-tri for simulated plot, as-synthesized sample, and sample after immersing in water for 2 days and 4 days.

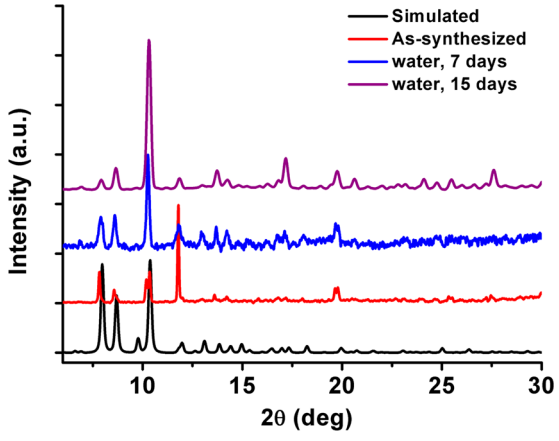

Figure 4. PXRD patterns of **rht**-MOF-pyr for simulated plot, as-synthesized sample, and sample after immersing in water for 7 days and 15 days.

stability: pyrazolate > triazolate > tetrazolate in terms of stabilizing the copper paddlewheel MBBs against water. This is in good agreement with the increasing pK_a values of these functional groups.[24−26]

We evaluated the moisture and steam stabilities of **rht**-MOF-tri and **rht**-MOF-pyr. As shown in Figure 5, the exposure of **rht**-MOF-tri to ambient air with a relative humidity of ∼70% for a week did not result in any observable structural change, and **rht**-MOF-tri was observed to retain crystallinity after exposure to steam (100% at 100 °C) for 6 h. No significant loss of crystallinity was observed for **rht**-MOF-pyr after similar tests (Figure 6).

We also examined the tolerance of **rht**-MOF-tri and **rht**-MOF-pyr to acidic media, a more stringent challenge for most MOFs. Soaking **rht**-MOF-tri in hydrochloric acid (HCl) aqueous solution with a pH of 2.5 for 24 h did not lead to observable structural change; however, dramatic loss of crystallinity was observed by extending the soaking time to 48 h (Figure 7). **rht**-MOF-tri exposed to pH = 1 HCl aqueous solution led to complete degradation of the framework (Figure 7). In contrast to **rht**-MOF-tri, **rht**-MOF-pyr survived in pH = 2.5 HCl aqueous solution for more than 1 week and even

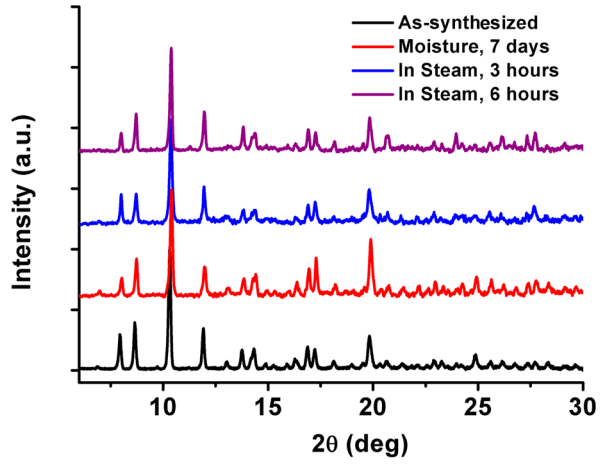

Figure 5. PXRD patterns of **rht**-MOF-tri for as-synthesized sample and samples after moisture and steam tests.

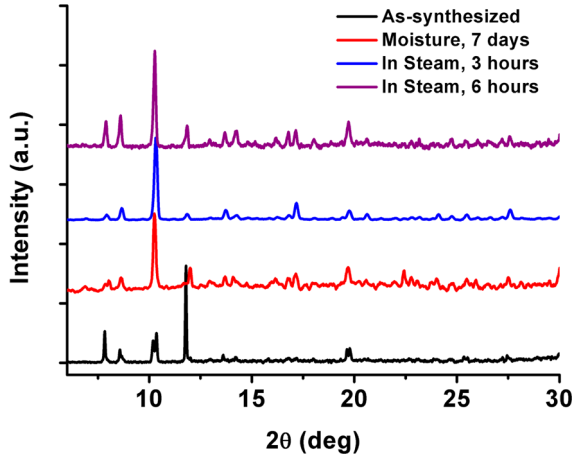

Figure 6. PXRD patterns of **rht**-MOF-pyr for as-synthesized sample and samples after moisture and steam tests.

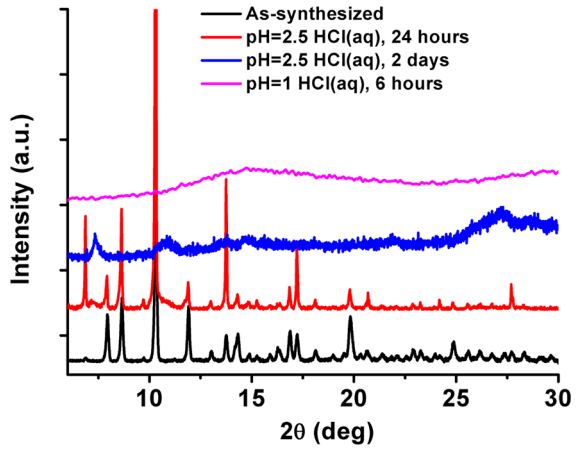

Figure 7. PXRD patterns of **rht**-MOF-tri for as-synthesized sample and samples after acid stability tests.

retained its crystallinity after 14 days (Figure 8). However, **rht**-MOF-pyr did not survive in pH = 1 HCl aqueous solution. These results indicate the relatively high chemical stability of **rht**-MOF-tri and **rht**-MOF-pyr compared with most other MOFs and suggest that the pyrazole group strongly promotes the tolerance of the **rht**-MOF platform toward acidic media.

DOI: 10.1021/acs.chemmater.5b00084
Chem. Mater. 2015, 27, 2144−2151

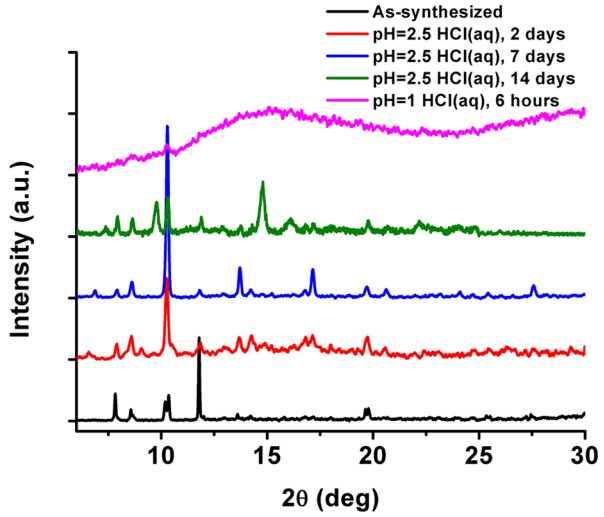

Figure 8. PXRD patterns of **rht**-MOF-pyr for as-synthesized sample and samples after acid stability tests.

Assessment of Surface Areas after Water/Chemical Stability Tests. Although PXRD has been extensively utilized to evaluate the preservation of crystalline structures for MOFs after water/chemical stability tests, recent studies have suggested that PXRD cannot detect partial structure loss and the surface area should be measured to validate the preservation of framework integrity.[13a] N_2 adsorption isotherms at 77 K were measured by reactivating **rht**-MOF-tri and **rht**-MOF-pyr samples after each stability test. As shown in Figure 9, **rht**-MOF-tri and **rht**-MOF-pyr retained their surface areas (Table 2) after various tests, confirming their water, moisture, steam, and chemical stability. **rht**-MOF-tri and **rht**-MOF-pyr represent two rare examples of highly porous MOFs that have been shown to be stable under water, moisture, steam, and acid conditions without significant loss of surface area.[16,17]

Analysis of Structure–Property Relationship for Water/Chemical Stability. The differences in properties among **rht**-MOF-1, **rht**-MOF-tri, and **rht**-MOF-pyr triggered by substitution of functional groups can presumably be attributed to the different properties of tetrazole, 1,2,3-triazole, and pyrazole. Since the N atom has an electron-withdrawing effect, an azolate ring containing less N atoms has higher basicity or lower acidity, leading to a high pK_a value. The pK_a of tetrazole is ca. 4.6, meaning that it is a relatively weak chelating ligand.[24] In contrast, the pK_a of 1,2,3-triazole is ca. 9.3,[25] and that of pyrazole is ca. 14.0.[26] As investigated by Long's and Chen's groups,[16,22] the pK_a value or basicity of the ligand can be regarded as a straightforward measure of binding ability toward a proton and may also be applied to estimate the bonding strength with transition metal ions. The increase in basicity of the azolate groups presumably increases the Cu–N bond strength, which is supported by Cu–N bond distances of 1.952, 1.937, and 1.931 Å in **rht**-MOF-1, **rht**-MOF-tri, and **rht**-MOF-pyr, respectively. The change in the bonding of the triangular inorganic MBB, $[Cu_3O(N_{4-x}(CH)_xC-)_3]$ (x = 0, 1, or 2), is in a direct relationship with the bonding of the copper paddlewheel SBU (i.e., remotely strengthening the Cu–carboxylate bonding), thus exerting changes in the electronic structure of the whole MOF to afford different stabilities toward water.

Computational Studies. To gain insight into the changes in water/chemical stabilities, we performed computational studies[14a] on these three **rht**-MOFs. Analysis of the electronic structures for all three **rht**-MOFs revealed a few noticeable differences in the partial charges between the structures, especially in the five-membered rings (see the Supporting Information). Note that the partial charges referenced here were calculated using the Connolly charge-fitting scheme[27] (see the Supporting Information). In **rht**-MOF-1, the uncoordinated nitrogen atoms on the tetrazolate group are highly electronegative with a partial charge of about −0.5 e^-, while the coordinated nitrogen atoms (those that are bonded to the Cu^{2+} ions of the triangular inorganic MBB) are less electronegative with a partial charge of about −0.2 e^-. For the 1,2,3-triazolate moiety of **rht**-MOF-tri, when comparing to the tetrazolate group in **rht**-MOF-1, it can be seen that replacing one the

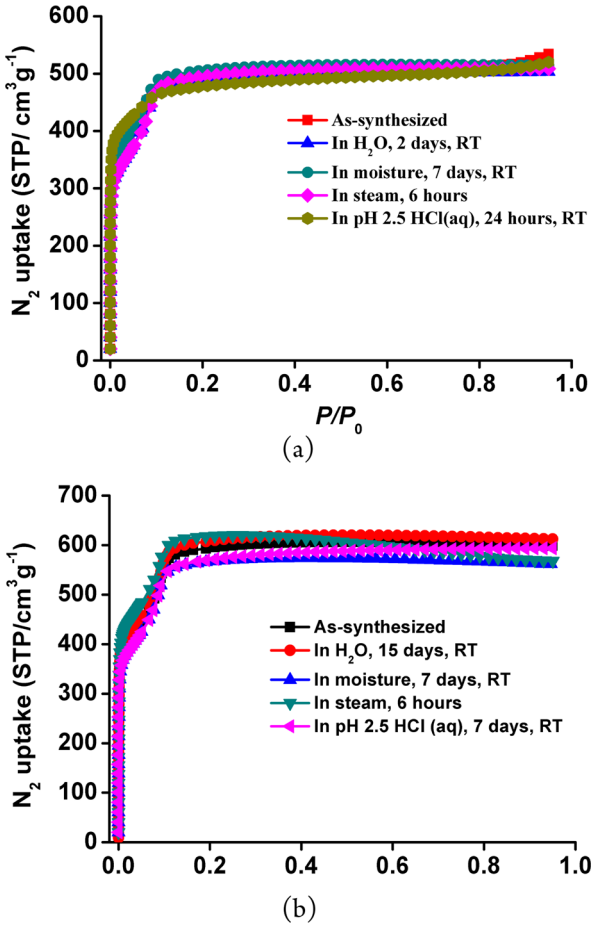

Figure 9. N_2 adsorption isotherms at 77 K for (a) **rht**-MOF-tri; (b) **rht**-MOF-pyr.

Table 2. Surface Areas for rht-MOF-tri and rht-MOF-pyr: As-Synthesized and after Treatment with Water, Moisture, Steam, and $HCl_{(aq)}$ at pH 2.5[a]

conditions	**rht**-MOF-tri $SA_{BET}/m^2\ g^{-1}$	**rht**-MOF-pyr $SA_{BET}/m^2\ g^{-1}$
as-synthesized	1841(31)	2133(62)
moisture	1818(26)	2183(64)
H_2O	1874(44)	2049(65)
steam	1803(23)	2261(57)
pH 2.5 $HCl_{(aq)}$	1812(10)	2050(66)

[a]Values were obtained from N_2 adsorption measurements performed at 77 K on samples subjected to the conditions specified and then activated according to the procedures in the Experimental Section.

DOI: 10.1021/acs.chemmater.5b00084
Chem. Mater. 2015, 27, 2144–2151

uncoordinated nitrogen atoms with a C−H group causes one of the coordinated nitrogen atoms (the atom on the uncoordinated N atom side) to lose some electron density while the nearby coordinated N atom gains electron density. The uncoordinated nitrogen atom in **rht**-MOF-tri has a similar partial charge to those in **rht**-MOF-1. This increase in negative charge for the coordinated nitrogen atom on the C−H side of the 1,2,3-triazolate group presumably leads to stronger Cu−N bonds. In **rht**-MOF-pyr, the replacement of both uncoordinated nitrogen atoms with a C−H group causes both coordinated N atoms to gain electron density relative to those that are in the tetrazolate and 1,2,3-triazolate moieties of **rht**-MOF-1 and **rht**-MOF-tri, respectively; the partial charges for these nitrogen atoms are approximately −0.4 e^-. This electron density difference could be responsible for the enhanced stability of the trigonal $[Cu_3O(N_2(CH)_2C-)_3]$ units in **rht**-MOF-pyr with respect to the corresponding trigonal $[Cu_3O(N_3(CH)C-)_3]$ units in **rht**-MOF-tri and trigonal $[Cu_3O(N_4C-)_3]$ units in **rht**-MOF-1.

The substitution of tetrazolate with triazolate and pyrazolate moieties has also affected the copper paddlewheel units in the respective **rht**-MOFs. It is noteworthy that the two Cu^{2+} ions in the paddlewheels of **rht**-MOFs are indeed chemically distinct, as the carboxylate carbon−aromatic carbon bond cannot rotate freely in the MOF. The Cu^{2+} ion labeled 1 in Figures S4−S6 (Supporting Information), denoted herein as Cu1, faces toward the center of the linker and projects into the truncated tetrahedral cage, and the Cu^{2+} ion labeled 2, denoted herein as Cu2, faces away from the center of the linker and projects into the cuboctahedral cage. The relative partial charges about the Cu^{2+} ions have been shown to be significant in **rht**-MOFs, with the more positively charged Cu^{2+} ion acting as the favored sorption site.[28] Electronic structure calculations show that the Cu1 ions have the higher charge within the paddlewheels in **rht**-MOF-1 and **rht**-MOF-tri; this can be attributed to the presence of the proximal uncoordinated nitrogen atoms on the five-membered rings in both **rht**-MOFs, which causes the partial positive charge of the Cu1 ions to increase relative to the Cu2 ions. This can be interpreted as a consequence of the repulsive interaction between the electronegative uncoordinated nitrogen atoms and the electronic environment of the copper paddlewheels in these two **rht**-MOFs, causing the electron density to shift toward the more distant Cu2 ions. In **rht**-MOF-pyr, the replacement of all uncoordinated N atoms with C−H groups shifts the higher positive charge to the Cu2 ion and thereby increases the electron density of the Cu1 ions. Therefore, in **rht**-MOF-pyr, the Cu1 ions, which are in closer proximity to the attractive triangular inorganic MBB, are less favorable toward sorbate molecules, such as water.

The potential energy surface (PES) was generated for the copper paddlewheel $[Cu_2(O_2C-)_4]$ fragments in all three **rht**-MOFs. The results revealed that the bond energies are lower and produced a deeper well-depth for **rht**-MOF-tri and **rht**-MOF-pyr compared to **rht**-MOF-1 (Figure 10). This would be expected to afford enhanced stability for the copper paddlewheel units in **rht**-MOF-tri and **rht**-MOF-pyr. Indeed, it can be observed in Figure 10 that the Cu^{2+}−O interactions of the copper paddlewheels (considering both types of paddlewheel Cu^{2+} ions) are more stable for **rht**-MOF-pyr and **rht**-MOF-tri compared to those for **rht**-MOF-1 by approximately 38 and 30 kJ·mol^{-1}, respectively. In effect, enhanced bonding between the pyrazolate groups and the triangular inorganic MBB synergistically stabilized the copper paddlewheel MBBs in both **rht**-MOF-pyr and **rht**-MOF-tri. These computational findings support the experimentally observed increase in water stability from **rht**-MOF-1 to **rht**-MOF-tri, and to **rht**-MOF-pyr.

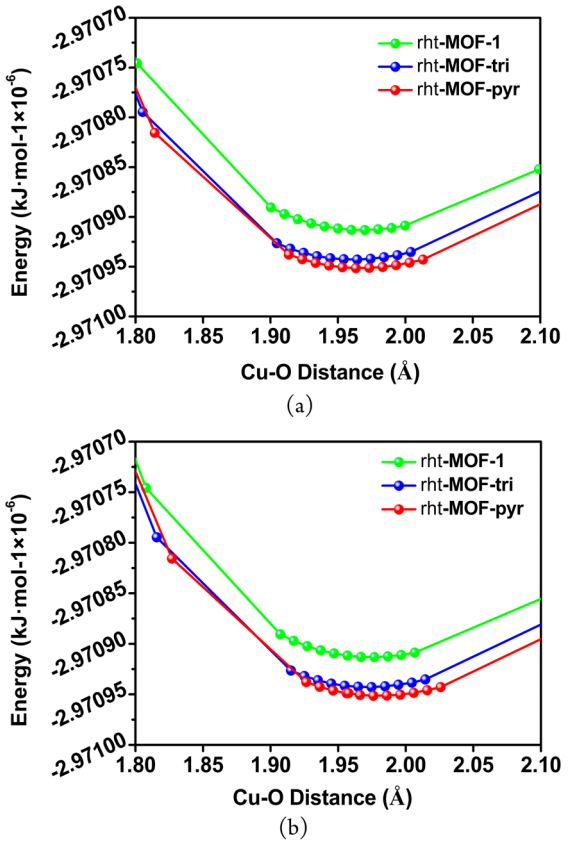

Figure 10. Generated potential energy surfaces about (a) the Cu1 ions (atom labeled 1 in Figures S4−S6, Supporting Information) and (b) the Cu2 ions (atom labeled 2 in Figures S4−S6) of the copper paddlewheels for **rht**-MOF-1 (green), **rht**-MOF-tri (blue), and **rht**-MOF-pyr (red).

CONCLUSION

In summary, we demonstrated how to stabilize the copper paddlewheel MBBs, $[Cu_2(O_2C-)_4]$, via a crystal engineering approach that enables strengthening the bonding between the organic ligands and the triangular inorganic MBB, $[Cu_3O(N_{4-x}(CH)_xC-)_3]$ (x = 0, 1, or 2), which, in turn, remotely enhances the stability of the copper paddlewheel MBB. The observed experimental results are further supported by computational studies, which allowed for a better understanding of the mechanism promoting the copper paddlewheel stability. Therefore, this study paves the way to the synthesis and development of prospective suitable MOFs with enhanced water stability.

EXPERIMENTAL SECTION

General Information. All of the reagents were obtained from commercial vendors and, unless otherwise noted, were used without further purification.

Synthesis of 5-(1*H*-1,2,3-Triazol-4-yl)isophthalic Acid (H_3TAIP). Dimethyl 5-iodoisophthalate (1 mmol) and ethynyltrimethylsilane (2 mmol) were suspended in a solution of 50 mL of dry tetrahydrofuran (THF) and 5 mL of triethylamine (Et_3N) under a nitrogen atmosphere. Tetrakis(triphenylphosphine) palladium ($Pd(PPh_3)_4$) (0.005 mmol) and copper(I) iodide (CuI) (0.015 mmol) were then added. The reaction mixture was stirred for 12 h at 60 °C

DOI: 10.1021/acs.chemmater.5b00084
Chem. Mater. 2015, 27, 2144−2151

and subsequently evaporated and chromatographed (silica gel, EtOAc/hexane = 1:60) to give the product as a yellow solid (91% yield). The detailed procedure of preparation of dimethyl 5-(1-(pivaloyloxymethyl)-1*H*-1,2,3-triazol-4-yl)isophthalate can be found in the reported reference (yield: 97%).[29] To a solution of dimethyl 5-(1-(pivaloyloxymethyl)-1*H*-1,2,3-triazol-4-yl) isophthalate (1 mmol) in THF/H_2O (1:1, 10 mL) was added LiOH (10 mmol), and the mixture was then stirred at room temperature for 12 h. The mixture was neutralized with a 1 M HCl solution to pH = 5. The resulting precipitate was filtered, washed with 10 mL of water, and dried under vacuum to produce the pure product 5-(1*H*-1,2,3-triazol-4-yl) isophthalic acid, which is a white solid (yield: 86%) (^{1}H NMR, D_2O, 250 MHz, δ = 8.28 (2H), 8.15(1H), 8.02 (1H)).

Synthesis of 5-(1*H*-Pyrazol-4-yl)isophthalic Acid (H_3PAIP). 4-Bromo-1-trityl-1*H*-pyrazole and 3,5-bis(methoxycarbonyl)-phenylboronic acid were synthesized by the procedures reported in the literatures.[30] The mixture of 4-bromo-1-trityl-1*H*-pyrazole (1.39 g, 3.56 mmol), 3,5-bis(methoxycarbonyl)phenylboronic acid (0.93 g, 3.91 mmol), tetrakis(triphenylphosphine) palladium (0.42 g, 0.36 mmol), and K_2CO_3 (0.98 g, 7.12 mmol) in a 100 mL recovery flask was added into 1,2-dimethoxyethane (18 mL) and H_2O (10 mL) under nitrogen protection. The reaction mixture was heated at 85 °C and stirred for 36 h. After 36 h, the reaction mixture was concentrated on a rotary evaporator. The residue was taken up in EtOAc (50 mL), washed with H_2O (15 mL), and dried ($MgSO_4$). After filtration, the filtrate was concentrated on a rotary evaporator. The crude product was hydrolyzed by KOH solution in THF/MeOH/H_2O (v1/1/2) mixture solvents. The reaction mixture was then concentrated on a rotary evaporator and acidified by conc. HCl. The collected solid was dissolved in dichloromethane, and several drops of trifluoroacetic acid were added into the solution to deprotect trityl group. The reaction mixture was warmed to 40 °C overnight. 5-(1*H*-Pyrazol-4-yl)-isophthalic acid (H_3PAIP) was collected by filtration (yield: 50%) (^{1}HNMR, [D_6]DMSO, 250 MHz, δ = 8.35 (2H), 8.29(1H), 8.25 (2H)).

Synthesis of rht-MOF-tri. A mixture of 5-(1*H*-1,2,3-triazoyl) isophthalic acid (H_3TAIP) (30 mg), $CuNO_3{\cdot}2.5H_2O$ (90 mg), and *N*,*N*′-dimethylformamide (DMF) (1.5 mL) with 2 drops of HBF_4 (47% aqueous) was added into a 4 mL vial and then heated to 65 °C for 48 h. The resulting octahedron-shaped green crystals were obtained (yield: 75% based on H_3TAIP ligand).

Synthesis of rht-MOF-pyr. A mixture of 5-(1*H*-pyrazol-4-yl)isophthalic acid (H_3PAIP) (10 mg), $CuNO_3{\cdot}2.5H_2O$ (30 mg), and *N*,*N*′-dimethylformamide (DMF) (1.0 mL) with 2 drops of HBF_4 (47% aqueous) was added into a 4 mL vial and then heated to 70 °C for 48 h. The resulting octahedron-shaped green crystals were obtained (yield: 70% based on H_3PAIP ligand).

■ ASSOCIATED CONTENT

Ⓢ Supporting Information

Full experimental details, calculation results, and other data. This material is available free of charge via the Internet at http://pubs.acs.org.

■ AUTHOR INFORMATION

Corresponding Authors

*E-mail: sqma@usf.edu (S.M.).
*E-mail: xiaodong.shi@mail.wvu.edu (X.S.).
*E-mail: mohamed.eddaoudi@kaust.edu.sa (M.E.).

Notes

The authors declare no competing financial interest.

■ ACKNOWLEDGMENTS

The authors acknowledge NSF (DMR-1352065) and USF for financial support of this work. B.S. acknowledges the National Science Foundation (Award No. CHE-1152362), the computational resources that were made available by an XSEDE Grant (No. TG-DMR090028), and the use of the services provided by Research Computing at the University of South Florida. X.S. thanks NSF for the financial support (CHE-0844602). The single-crystal X-ray diffraction of **rht**-MOF-tri and **rht**-MOF-pyr was carried out at the Advanced Photon Source on beamline 15-ID-B of ChemMatCARS Sector 15, supported by the National Science Foundation under grant number NSF/CHE-1346572. This research used resources of the Advanced Photon Source, a U.S. Department of Energy (DOE) Office of Science User Facility operated for the DOE Office of Science by Argonne National Laboratory under Contract No. DE-AC02-06CH11357. M.E. acknowledges the financial support from King Abdullah University of Science and Technology.

■ REFERENCES

(1) (a) Zhou, H.-C.; Long, J. R.; Yaghi, O. M. *Chem. Rev.* **2012**, *112*, 673. (b) Zhou, H.-C.; Kitagawa, S. *Chem. Soc. Rev.* **2014**, *43*, 5415.

(2) (a) Desiraju, G. R. *Angew. Chem., Int. Ed.* **2007**, *46*, 8342. (b) Zheng, S.-T.; Wu, T.; Irfanoglu, B.; Zuo, F.; Feng, P.; Bu, X. *Angew. Chem., Int. Ed.* **2011**, *50*, 8034. (c) Mallick, A.; Garai, B.; Díaz, D.; Banerjee, R. *Angew. Chem., Int. Ed.* **2013**, *52*, 13755. (d) Yaghi, O. M.; O'Keeffe, M.; Ockwig, N. W.; Chae, H. K.; Eddaoudi, M.; Kim, J. *Nature* **2003**, *423*, 705−714.

(3) (a) Perry, J. J.; Perman, J. A.; Zaworotko, M. J. *Chem. Soc. Rev.* **2009**, *38*, 1400. (b) Furukawa, H.; Cordova, K. E.; O'Keeffe, M.; Yaghi, O. M. *Science* **2013**, *341*, 1230444. (c) Guillerm, V.; Kim, D.; Eubank, J. F.; Luebke, R.; Liu, X.; Adil, K.; Lah, M. S.; Eddaoudi, M. *Chem. Soc. Rev.* **2014**, *43*, 6141. (d) Lu, W.; Wei, Z.; Gu, Z.-Y.; Liu, T.-F.; Park, J.; Park, J.; Tian, J.; Zhang, M.; Zhang, Q.; Gentle, T.; Bosch, M.; Zhou, H.-C. *Chem. Soc. Rev.* **2014**, *43*, 5561. (e) Guillerm, V.; Weseliński, Ł. J.; Belmabkhout, Y.; Cairns, A. J.; D'Elia, V.; Wojtas, L.; Adil, K.; Eddaoudi, M. *Nat. Chem.* **2014**, *6*, 673. (f) Gao, W.-Y.; Ma, S. *Comments Inorg. Chem.* **2014**, *34*, 125.

(4) (a) Ma, S.; Zhou, H.-C. *Chem. Commun.* **2010**, *46*, 44. (b) Suh, M. P.; Park, H. J.; Prasad, T. K.; Lim, D.-W. *Chem. Rev.* **2012**, *112*, 782. (c) He, Y.; Zhou, W.; Qian, G.; Chen, B. *Chem. Soc. Rev.* **2014**, *43*, 5657.

(5) (a) Li, J.-R.; Sculley, J.; Zhou, H.-C. *Chem. Rev.* **2012**, *112*, 869. (b) Sumida, K.; Rogow, D. L.; Mason, J. A.; McDonald, T. M.; Bloch, E. D.; Herm, Z. R.; Bae, T.-H.; Long, J. R. *Chem. Rev.* **2012**, *112*, 724. (c) Barea, E.; Montoro, C.; Navarro, J. A. R. *Chem. Soc. Rev.* **2014**, *43*, 5419.

(6) (a) Nugent, P.; Belmabkhout, Y.; Burd, S. D.; Cairns, A. J.; Luebke, R.; Forrest, K.; Pham, T.; Ma, S.; Space, B.; Wojtas, L.; Eddaoudi, M.; Zaworotko, M. J. *Nature* **2013**, *495*, 80. (b) Li, J.-R.; Ma, Y.; McCarthy, M. C.; Sculley, J.; Yu, J.; Jeong, H.-K.; Balbuena, P. B.; Zhou, H.-C. *Coord. Chem. Rev.* **2011**, *255*, 1791.

(7) (a) Kreno, L. E.; Leong, K.; Farha, O. K.; Allendorf, M.; Van Duyne, R. P.; Hupp, J. T. *Chem. Rev.* **2012**, *112*, 1105. (b) Cui, Y.; Yue, Y.; Qian, G.; Chen, B. *Chem. Rev.* **2012**, *112*, 1126. (c) Hu, Z.; Deibert, B. J.; Li, J. *Chem. Soc. Rev.* **2014**, *43*, 5815.

(8) (a) Yoon, M.; Srirambalaji, R.; Kim, K. *Chem. Rev.* **2012**, *112*, 1196. (b) Dhakshinamoorthy, A.; Garcia, H. *Chem. Soc. Rev.* **2014**, *43*, 5750. (c) Liu, J.; Chen, L.; Cui, H.; Zhang, J.; Zhang, L.; Su, C.-Y. *Chem. Soc. Rev.* **2014**, *43*, 6011.

(9) (a) Cohen, S. M. *Chem. Rev.* **2012**, *112*, 970. (b) Gao, W.-Y.; Chrzanowski, M.; Ma, S. *Chem. Soc. Rev.* **2014**, *43*, 5841. (c) Stavila, V.; Talin, A. A.; Allendorf, M. D. *Chem. Soc. Rev.* **2014**, *43*, 5994. (d) Ramaswamy, P.; Wong, N. E.; Shimizu, G. K. H. *Chem. Soc. Rev.* **2014**, *43*, 5913.

(10) Chui, S. S.-Y.; Lo, S. M.-F.; Charmant, J. P. H.; Orpen, A. G.; Williams, I. D. *Science* **1999**, *283*, 1148.

(11) Chen, B.; Ockwig, N. W.; Millward, A. R.; Contreras, D. S.; Yaghi, O. M. *Angew. Chem., Int. Ed.* **2005**, *44*, 4745.

(12) Nouar, F.; Eubank, J. F.; Bousquet, T.; Wojtas, L.; Zaworotko, M. J.; Eddaoudi, M. *J. Am. Chem. Soc.* **2008**, *130*, 1833.

DOI: 10.1021/acs.chemmater.5b00084
Chem. Mater. 2015, 27, 2144−2151

(13) (a) Schoenecker, P. M.; Carson, C. G.; Jasuja, H.; Flemming, C. J. J.; Walton, K. S. *Ind. Eng. Chem. Res.* **2012**, *51*, 6513. (b) Jasuja, H.; Burtch, N. C.; Huang, Y.-G.; Cai, Y.; Walton, K. S. *Langmuir* **2013**, *29*, 633.
(14) (a) Greathouse, J. A.; Allendorf, M. D. *J. Am. Chem. Soc.* **2006**, *128*, 10678. (b) Cychosz, K. A.; Matzger, A. J. *Langmuir* **2010**, *26*, 17198.
(15) (a) Taylor, J. M.; Vaidhyanathan, R.; Iremonger, S. S.; Shimizu, G. K. H. *J. Am. Chem. Soc.* **2012**, *134*, 14338. (b) Low, J. J.; Benin, A. I.; Jakubczak, P.; Abrahamian, J. F.; Faheem, S. A.; Willis, R. R. *J. Am. Chem. Soc.* **2009**, *131*, 15834. (c) Li, T.; Chen, D.-L.; Sullivan, J. E.; Kozlowski, M. T.; Johnson, J. K.; Rosi, N. L. *Chem. Sci.* **2013**, *4*, 1746.
(16) (a) Demessence, A.; D'Alessandro, D. M.; Foo, M. L.; Long, J. R. *J. Am. Chem. Soc.* **2009**, *131*, 8784. (b) Choi, H. J.; Dincă, M.; Dailly, A.; Long, J. R. *Energy Environ. Sci.* **2010**, *3*, 117. (c) Colombo, V.; Galli, S.; Choi, H. J.; Han, G. D.; Maspero, A.; Palmisano, G.; Masciocchi, N.; Long, J. R. *Chem. Sci.* **2011**, *2*, 1311. (d) Jasuja, H.; Jiao, Y.; Burtch, N. C.; Huang, Y.-g.; Walton, K. S. *Langmuir* **2014**, *30*, 14300−14307.
(17) Sumida, K.; Rogow, D. L.; Mason, J. A.; McDonald, T. M.; Bloch, E. D.; Herm, Z. R.; Bae, T.-H.; Long, J. R. *Chem. Rev.* **2012**, *112*, 724.
(18) Gul-E-Noor, F.; Jee, B.; Pöppl, A.; Hartmann, M.; Himsl, D.; Bertmer, M. *Phys. Chem. Chem. Phys.* **2011**, *13*, 7783.
(19) Burtch, N. C.; Jasuja, H.; Walton, K. S. *Chem. Rev.* **2014**, *114*, 10575.
(20) Tan, K.; Nijem, N.; Canepa, P.; Gong, Q.; Li, J.; Thonhauser, T.; Chabal, Y. J. *Chem. Mater.* **2012**, *24*, 3153.
(21) (a) Zou, Y.; Park, M.; Hong, S.; Lah, M. S. *Chem. Commun.* **2008**, 2340. (b) Hong, S.; Oh, M.; Park, M.; Yoon, J. W.; Chang, J.-S.; Lah, M. S. *Chem. Commun.* **2009**, 5397. (c) Yan, Y.; Lin, X.; Yang, S.; Blake, A. J.; Dailly, A.; Champness, N. R.; Hubberstey, P.; Schroder, M. *Chem. Commun.* **2009**, 1025. (d) Zhao, D.; Yuan, D.; Sun, D.; Zhou, H.-C. *J. Am. Chem. Soc.* **2009**, *131*, 9186. (e) Yuan, D.; Zhao, D.; Sun, D.; Zhou, H.-C. *Angew. Chem., Int. Ed.* **2010**, *49*, 5357. (f) Yan, Y.; Telepeni, I.; Yang, S.; Lin, X.; Kockelmann, W.; Dailly, A.; Blake, A. J.; Lewis, W.; Walker, G. S.; Allan, D. R.; Barnett, S. A.; Champness, N. R.; Schroder, M. *J. Am. Chem. Soc.* **2010**, *132*, 4092. (g) Farha, O. K.; Yazaydın, O.; Eryazici, I.; Malliakas, C.; Hauser, B.; Kanatzidis, M. G.; Nguyen, S. T.; Snurr, R. Q.; Hupp, J. T. *Nat. Chem.* **2010**, *2*, 944. (h) Zheng, B.; Bai, J.; Duan, J.; Wojtas, L.; Zaworotko, M. J. *J. Am. Chem. Soc.* **2011**, *133*, 748. (i) Yan, Y.; Blake, A. J.; Lewis, W.; Barnett, S. A.; Dailly, A.; Champness, N. R.; Schroder, M. *Chem.—Eur. J.* **2011**, *17*, 11162. (j) Yuan, D.; Zhao, D.; Zhou, H.-C. *Inorg. Chem.* **2011**, *50*, 10528. (k) Luebke, R.; Eubank, J. F.; Cairns, A. J.; Belmabkhout, Y.; Wojtas, L.; Eddaoudi, M. *Chem. Commun.* **2012**, *48*, 1455. (l) Li, B.; Zhang, Z.; Li, Y.; Yao, K.; Zhu, Y.; Deng, Z.; Yang, F.; Zhou, X.; Li, G.; Wu, H.; Nijem, N.; Chabal, Y. J.; Lai, Z.; Han, Y.; Shi, Z.; Feng, S.; Li, J. *Angew. Chem., Int. Ed.* **2012**, *51*, 1412. (m) Zheng, B.; Yang, Z.; Bai, J.; Li, Y.; Li, S. *Chem. Commun.* **2012**, *48*, 7025. (n) Farha, O. K.; Wilmer, C. E.; Eryazici, I.; Hauser, B. G.; Parilla, P. A.; O'Neill, K.; Sarjeant, A. A.; Nguyen, S. T.; Snurr, R. Q.; Hupp, J. T. *J. Am. Chem. Soc.* **2012**, *134*, 9860. (o) Farha, O. K.; Eryazici, I.; Jeong, N. C.; Hauser, B. G.; Wilmer, C. E.; Sarjeant, A. A.; Snurr, R. Q.; Nguyen, S. T.; Yazaydın, A. O.; Hupp, J. T. *J. Am. Chem. Soc.* **2012**, *134*, 15016. (p) Zhao, X.-L.; Sun, D.; Yuan, S.; Feng, S.; Cao, R.; Yuan, D.; Wang, S.; Dou, J.; Sun, D. *Inorg. Chem.* **2012**, *51*, 10350. (q) Eubank, J. F.; Nouar, F.; Ryan, L.; Cairns, A. J.; Wojtas, L.; Alkordi, M.; Bousquet, T.; Hight, M. R.; Eckert, J.; Embs, J. P.; Georgiev, P. A.; Eddaoudi, M. *Angew. Chem., Int. Ed.* **2012**, *51*, 10099. (r) Eryazici, I.; Farha, O. K.; Hauser, B. G.; Yazaydın, A. O.; Sarjeant, A. A.; Nguyen, S. T.; Hupp, J. T. *Cryst. Growth Des.* **2012**, *12*, 1075. (s) Yan, Y.; Suyetin, M.; Bichoutskaia, E.; Blake, A. J.; Allan, D. R.; Barnett, S. A.; Schroder, M. *Chem. Sci.* **2013**, *4*, 1731. (t) Wilmer, C. E.; Farha, O. K.; Yildirim, T.; Eryazici, I.; Krungleviciute, V.; Sarjeant, A. A.; Snurr, R. Q.; Hupp, J. T. *Energy Environ. Sci.* **2013**, *6*, 1158. (u) Wang, X.-J.; Li, P.-Z.; Chen, Y.; Zhang, Q.; Zhang, H.; Chan, X. X.; Ganguly, R.; Li, Y.; Jiang, J.; Zhao, Y. *Sci. Rep.* **2013**, *3*, 1149. (v) Luebke, R.; Weselinski, L. J.; Belmabkhout, Y.; Chen, Z.; Wojtas, L.; Eddaoudi, M. *Cryst. Growth Des.* **2014**, *14*, 414. (w) Barin, G.; Krungleviciute, V.; Gomez-Gualdron, D. A.; Sarjeant, A. A.; Snurr, R. Q.; Hupp, J. T.; Yildirim, T.; Farha, O. K. *Chem. Mater.* **2014**, *26*, 1912. (x) Liu, K.; Li, B.; Li, Y.; Li, X.; Yang, F.; Zeng, G.; Peng, Y.; Zhang, Z.; Li, G.; Shi, Z.; Feng, S.; Song, D. *Chem. Commun.* **2014**, *50*, 5031. (y) Liu, K.; Ma, D.; Li, B.; Li, Y.; Yao, K.; Zhang, Z.; Han, Y.; Shi, Z. *J. Mater. Chem. A* **2014**, *2*, 15823.
(22) Zhang, J.-P.; Zhang, Y.-B.; Lin, J.-B.; Chen, X.-M. *Chem. Rev.* **2012**, *112*, 1001.
(23) Spek, A. L. *J. Appl. Crystallogr.* **2003**, *36*, 7.
(24) McManus, J. M.; Herbst, R. M. *J. Org. Chem.* **1959**, *24*, 1643.
(25) Bordwell, F. G. *Acc. Chem. Res.* **1988**, *21*, 456.
(26) Catalan, J.; Abboud, J. L.; Elguero, J. *Adv. Heterocycl. Chem.* **1987**, *41*, 187.
(27) Singh, U. C.; Kollman, P. A. *J. Comput. Chem.* **1984**, *5*, 129.
(28) (a) Forrest, K. A.; Pham, T.; McLaughlin, K.; Belof, J. L.; Stern, A. C.; Zaworotko, M. J.; Space, B. *J. Phys. Chem. C* **2012**, *116*, 15538. (b) Pham, T.; Forrest, K. A.; Nugent, P.; Belmabkhout, Y.; Luebke, R.; Eddaoudi, M.; Zaworotko, M. J.; Space, B. *J. Phys. Chem. C* **2013**, *117*, 9340. (c) Pham, T.; Forrest, K. A.; Hogan, A.; McLaughlin, K.; Belof, J. L.; Eckert, J.; Space, B. *J. Mater. Chem. A* **2014**, *2*, 2088.
(29) Loren, J. C.; Krasinski, A.; Fokin, V. V.; Sharpless, K. B. *Synlett* **2005**, *18*, 2847.
(30) (a) Anderson, E. D.; Boger, D. L. *J. Am. Chem. Soc.* **2011**, *133*, 12285. (b) Kumar, A. B.; Anderson, J. M.; Manetsch, R. *Org. Biomol. Chem.* **2011**, *9*, 6284.

DOI: 10.1021/acs.chemmater.5b00084
Chem. Mater. 2015, 27, 2144−2151